Nonclassical light generation via a four-level inverted-Y system

Jianming Wen,[1,*] Shengwang Du,[2] Yanpeng Zhang,[3] Min Xiao,[3] and Morton H. Rubin[1]
[1]*Physics Department, University of Maryland, Baltimore County, Baltimore, Maryland 21250, USA*
[2]*Edward L. Ginzton Laboratory, Stanford University, Stanford, California 94305, USA*
[3]*Department of Physics, University of Arkansas, Fayetteville, Arkansas 72701, USA*
(Received 19 November 2007; published 7 March 2008)

We have theoretically analyzed nonclassical paired photons generated spontaneously from a four-level inverted-Y atomic system. We discuss the feasibility of biphoton generation due to different pumping arrangements. Two types of correlated photon pair emissions have been carefully examined: dressed cascade and dressed double-Λ emissions. In the dressed cascade two-photon emission, the coincidence counting rate may exhibit a damped Rabi oscillation, in contrast with a simple exponential decay feature in the literatures. In the dressed double-Λ configuration, we show that not only is the temporal correlation of entangled Stokes–anti-Stokes photons in agreement with discussions presented by Wen *et al.* [Phys. Rev. A **76**, 013825 (2007)], but also the oscillation period may be manipulated by altering either the control Rabi frequency or the dressing Rabi frequency or both. All the observed damped Rabi oscillations in the two-photon coincidences result from the destructive interference among the possible four-wave mixing processes occurring in the atom-field interaction system. This feature of the two-photon amplitude is governed by the convolution between the phase matching and third-order nonlinear susceptibility. The methodology adopted here can be applied to other atomic-level configurations and provides a useful tool to study the spectroscopy of the system. The generated narrow-band photon pairs may have potential applications in long-distance quantum communication and quantum information processing.

DOI: 10.1103/PhysRevA.77.033816 PACS number(s): 42.50.Dv, 42.65.Lm, 42.65.An, 32.80.−t

I. INTRODUCTION

Since the early days of nonlinear optics, there has been substantial interest in utilizing resonant atomic and molecular systems for efficient nonlinear optical processes. Unfortunately, attempts to use this resonance enhancement have been frustrated by problems associated with resonant absorption, phase shifts, and unwanted nonlinearities. Over the last ten years, both theoretical and experimental work have challenged this paradigm—nonlinear optics at resonance by using the technique of electromagnetically induced transparency (EIT) [1]. By utilizing this technique, the resonant nonlinear optical processes have been even demonstrated in the very low-light level (e.g., [2]). Recently, entangled photon pairs have been generated by further pushing the resonant nonlinear optics into the two-photon limit [3–5].

Compared with the conventional paired photons produced from spontaneous parametric down-conversion (SPDC) [6,7], correlated photons produced from the atomic ensemble have properties such as narrow spectral width, long coherence time and long coherence length, high spectral brightness, and high conversion efficiency. These optical properties of the new entangled-photon source may have applications in long-distance quantum communication and quantum information processing. The properties of the new biphoton source, paired Stokes–anti-Stokes photons generated from a double-Λ EIT system, have been theoretically and experimentally studied in [3,4,8–12], including three-level [4,9,10] and four-level [3,8,11,12] atomic configurations. It was shown that the two-photon amplitude is a convolution of the phase matching function and the third-order nonlinear susceptibility [10]. Further, the properties of these correlated photons can be changed by manipulating the phase matching function and/or the third-order nonlinear susceptibility. By comparing the natural spectral width from the phase matching with the resonant linewidths from the third-order nonlinearity, the two-photon temporal correlation will exhibit a feature of either a square-wave-like pattern (same as in the conventional SPDC case) or damped Rabi oscillations, or in between. These damped Rabi oscillations are due to destructive interference between two possible four-wave mixing (FWM) processes which may not be resolved by detectors. If the detector could distinguish the generated modes, a simple exponential decay would replace the damped Rabi oscillations and the interference between two FWM processes would disappear. If the phase matching plays a dominant role in determining the coherence time of paired photons, the detailed generation mechanism of the two FWM processes will be erased because of the narrower spectral width set by the phase matching. In such a situation, a square-wave-like pattern will be observed in the two-photon coincidences. Subnatural-linewidth paired photons [13] can occur under such a condition in a high-optical-depth medium. Because of the EIT, the anti-Stokes photons resonant with the atomic transition can propagate through the medium with negligible absorption and a controllable slow group velocity.

A recent study of biphotons created from a two-level atomic system shows that in the spontaneous emission regime, the nonlinear coupling coefficients for the coupled field-operator equations are different from those for the classical FWM coupled field equations [5,14]. With the use of paired photons produced from a two-level system, a new two-photon beating experiment has been proposed in the resonant pumping case [15]. The beating results from the

*jianming.wen@gmail.com

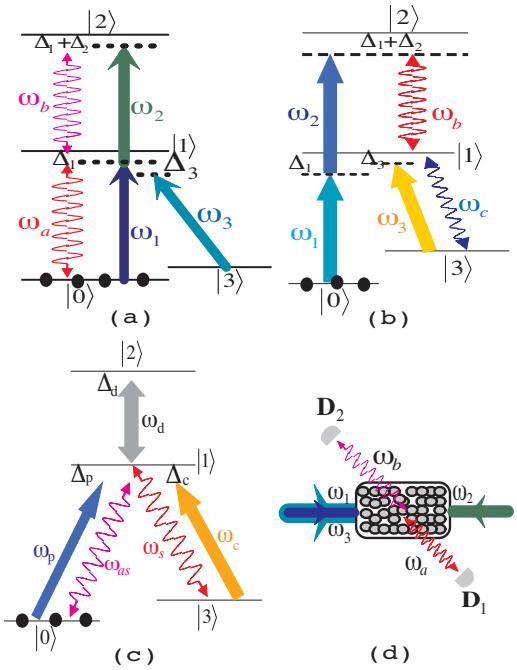

FIG. 1. (Color online) Mechanisms of biphoton generation from a four-level inverted-Y system and the backward detection geometry: (a) and (b) cascade paired-photon emitters, (c) dressed double-Λ paired Stokes–anti-Stokes generation, and (d) simplified backward detection geometry for cascade two-photon emission shown in (a). For notation, check the text.

different linear optical responses to two types of biphotons emitted in such a two-level system and the phenomenon has an analog with the Franson interferometer [16]. The two-photon beatings also provide another way to test the Bell inequality.

In this paper, the feasibility of another EIT-assisted entangled twin-photon source will be examined in the case of a four-level inverted-Y atomic system. The FWM and coexisting FWM and SWM (six-wave mixing) have been reported in recent experiments [17–19] implemented in such an inverted-Y configuration [20]. EIT not only enhances the signal generation, but also allows it to transmit through the atomic medium with small absorption. Compared with the previous double-Λ atomic configurations, it is shown that the flexible pumping arrangements allow for three types of biphoton generation in the inverted-Y atomic system. Paired photons may be generated either from the dressed cascade scheme or from the dressed double-Λ configuration, as shown in Figs. 1(a)–1(c). In the dressed cascade scheme, the analysis not only recovers the results which have been already presented in the literature [21,22], but also shows new phenomena. To entangle two cascade photons, it is indeed necessary to overlap their wave packets. We also find that the two-photon temporal correlation may have a damped Rabi oscillation rather than a simple exponential decay behavior [21,22]. The damped Rabi oscillation is the interference among possible FWM processes existing in the atom-photon interaction. If the coherence length is mainly determined by the phase matching, coincidences will become a square-wave-like pattern and all the modes generated in FWM processes cannot be spectrally resolved. In the dressed double-Λ configuration, we recover the previous conclusions about paired Stokes and anti-Stokes photons created in a three-level system [10]. The coincidence counting rate exhibits a damped Rabi oscillations or a square-wave-like feature and depends on whether the third-order nonlinearity or the phase matching is dominant in the two-photon amplitude. In addition, the oscillation period can be manipulated by changing either the control Rabi frequency or the dressing-laser Rabi frequency, or both. In both schemes of entangled-photon generation from such an inverted-Y system, the properties of the two-photon amplitude are governed by the convolution between the phase matching and the third-order nonlinear susceptibility.

The methodology of studying the atomic dynamics adopted here is the same as those used in [10,14,23,24]. This method offers a useful tool to look at the optical spectroscopy in the atom-photon interaction system and the atomic dynamics with other level configurations. The physics behind the two-photon temporal correlation is illustrated by using perturbation theory [7,8,10,14] which provides an intuitive picture of the biphoton optics. To include the effects of the absorption and gain in the propagation of generated fields, one resorts to the coupled Maxwell's equations as used in [3–5,8,9,11,12,22]. To simplify the discussions, the Doppler effect and Langevin noise terms will not be taken into account in the analysis. In the cooled atomic ensemble, the spectral broadening resulted from the Doppler effect is very small and negligible. Moreover, the polarization properties of generated photons are also neglected.

To focus on the mechanisms of paired photons generated from a four-level inverted-Y system, we organize the paper as follows. In Sec. II, two types of biphoton generation mechanisms in the inverted-Y atomic system will be discussed: the dressed cascade scheme and the dressed double-Λ configuration. We will analyze under what conditions paired photons may be generated through either the dressed cascade scheme or the dressed double-Λ configuration, or even both. Since the optical response plays a critical role in determining the feature of the two-photon temporal correlation, we will carefully evaluate both the linear and nonlinear optical responses to the generated fields. In Sec. III, we will concentrate on the two-photon temporal correlation for both schemes. To look at the optical properties of paired photons, perturbation theory will be used to calculate the two-photon amplitude. In particular, it is of interest to study the features of the coincidence counting rates in both schemes. The conclusions will be given in Sec. IV.

II. OPTICAL RESPONSE OF A FOUR-LEVEL INVERTED-Y SYSTEM

The optical response of the medium with a four-level inverted-Y configuration may lead to three possibilities for biphoton generation, as illustrated in Figs. 1(a)–1(c). Two possibilities correspond to generating paired photons via cascade two-photon schemes [Figs. 1(a) and 1(b)], and one corresponds to an addressed double-Λ configuration [Fig. 1(c)]. In this section, we will analyze the mechanisms and condi-

tions for producing biphotons from the cascade two-photon scheme and the dressed double-Λ configuration. We will concentrate on the optical responses to the generated fields in each mechanism.

The medium of interest is a (cooled) gas where identical four-level atoms or molecules are initially prepared in the ground level $|0\rangle$, see Figs. 1(a)–1(c). The idealized atoms or molecules are confined within a long thin cylindrical volume with a length L and cross-section area A. The averaged atomic density is N. For simplicity, we will ignore the Doppler effect [25] to the two-photon correlation throughout the paper, which will be discussed in another paper.

A. Cascade two-photon emitter

The two-photon spontaneous emission in a three-level atom in cascade configuration has been analyzed in [21], and further physical insights have been presented in [22]. The two-photon temporal correlation in the current scheme can exhibit different behavior from those obtained in [21,22]. An exponential decay feature is dominant in the two-photon coincidences in [21,22]; however, as shall be shown in Sec. II A, the two-photon joint detection in the current dressed cascade scheme can give a damped Rabi oscillation. In addition, the EIT effect is used to assist the propagation of the generated field by eliminating the absorption and manipulating the phase matching.

For the cascade paired-photon emitter considered here, we will take the case shown in Fig. 1(a) as an example. The analysis of biphotons created from the case depicted in Fig. 1(b) is similar. In Fig. 1(a), a weak pump beam with angular frequency ω_1 and a strong laser with angular frequency ω_2 are counterpropagating through the medium. Paired photons are spontaneously emitted into opposite directions. The weak pump field is tuned to the atomic transition $|0\rangle \rightarrow |1\rangle$ with detuning $\Delta_1 = \omega_{10} - \omega_1$ and a strong beam to the transition $|1\rangle \rightarrow |2\rangle$ with detuning $\Delta_2 = \omega_{21} - \omega_2$, where ω_{ij} is the transition frequency between levels $|i\rangle$ and $|j\rangle$. A dressing laser with angular frequency ω_3 is applied to the transition $|3\rangle \rightarrow |1\rangle$ with detuning $\Delta_3 = \omega_{13} - \omega_3$. The generated paired photons are peaking at frequencies $\omega_a = \omega_1 + \delta$ and $\omega_b = \omega_2 - \delta$, as indicated by wavy arrows in Fig. 1(a). The character of the FWM process is profoundly modified due to the strong intensities of the ω_2 field and the dressing ω_3 laser. In such a case, perturbation theory is not sufficient to describe the interaction between the medium and three input fields. In the photon-counting experiment, the backward geometry is chosen to set up two photodetectors D_1 and D_2; see Fig. 1(d). If $\vec{k}_1 + \vec{k}_2 = \vec{0}$ is well satisfied, the right-angle experimental scheme can be used to eliminate the background noise from the linear Rayleigh scattering of the ω_1 and ω_2 fields, where $\vec{k}_1$ and $\vec{k}_2$ are wave vectors. In such a case, the generated fields can trigger both detectors D_1 and D_2.

To study the dynamics of the atomic ensemble, we begin with the Heisenberg operator equations of motion in the dipole approximation:

$$\dot{\sigma}_{lm} = i\omega_{lm}\sigma_{lm} + i\sum_j (d_{mj}E\sigma_{lj} - d_{jl}E\sigma_{jm}), \tag{1}$$

where $\sigma_{lm} = |l\rangle\langle m|$ is the atomic operator, E is the total field operator, and $d_{mj} = \langle m|\vec{d}|j\rangle/\hbar$ is the dipole matrix element divided by $\hbar$. We write the positive-frequency field operators as follows:

$$E_{\mathrm{I}}^{(+)} e^{-i\omega_1 t} = [E_1 + E_a^{(+)} e^{-i\delta t}] e^{-i\omega_1 t},$$

$$E_{\mathrm{II}}^{(+)} e^{-i\omega_2 t} = [E_2 + E_b^{(+)} e^{i\delta t}] e^{-i\omega_2 t}, \tag{2}$$

where E_1 and E_2 represent the slowly varying amplitudes of two classical fields ω_1 and ω_2, and $E_a^{(+)}$ and $E_b^{(+)}$ are positive frequency parts of the generated field operators. The dressing laser ω_3 is also treated as a classical field E_3. To eliminate the fast phase oscillating terms in Eq. (1), the following transformations will be introduced:

$$Q_{ii} = \sigma_{ii} \quad (i = 0,1,2,3),$$

$$Q_{01} = \sigma_{01} e^{i\omega_1 t}, \quad Q_{12} = \sigma_{12} e^{i\omega_2 t}, \quad Q_{31} = \sigma_{31} e^{i\omega_3 t},$$

$$Q_{02} = \sigma_{02} e^{i(\omega_1+\omega_2)t}, \quad Q_{03} = \sigma_{03} e^{i(\omega_1-\omega_3)t}, \quad Q_{32} = \sigma_{32} e^{i(\omega_2+\omega_3)t}. \tag{3}$$

By plugging Eqs. (2) and (3) into (1), under the rotating-wave approximation one can obtain a set of equations which govern the atomic evolution:

$$\dot{Q}_{00} = -\gamma_0 Q_{00} + id_{01}E_{\mathrm{I}}^{(-)} Q_{01} - id_{10}E_{\mathrm{I}}^{(+)} Q_{10} + \mathcal{F}_{00},$$

$$\dot{Q}_{11} = -\gamma_1 Q_{11} + id_{10}E_{\mathrm{I}}^{(+)} Q_{10} - id_{01}E_{\mathrm{I}}^{(-)} Q_{01} + id_{12}E_{\mathrm{II}}^{(-)} Q_{12} - id_{21}E_{\mathrm{II}}^{(+)} Q_{21} + id_{13}E_3 Q_{13} - id_{31}E_3^* Q_{31} + \mathcal{F}_{11},$$

$$\dot{Q}_{22} = -\gamma_2 Q_{22} + id_{21}E_{\mathrm{II}}^{(+)} Q_{21} - id_{12}E_{\mathrm{II}}^{(-)} Q_{12} + \mathcal{F}_{22},$$

$$\dot{Q}_{33} = -\gamma_3 Q_{33} + id_{31}E_3^* Q_{31} - id_{13}E_3 Q_{13} + \mathcal{F}_{33},$$

$$\dot{Q}_{01} = -i\Gamma_{01} Q_{01} + id_{10}(Q_{00} - Q_{11})E_{\mathrm{I}}^{(+)} + id_{12}E_{\mathrm{II}}^{(-)} Q_{02} + id_{13}E_3 Q_{03} + \mathcal{F}_{01},$$

$$\dot{Q}_{12} = -i\Gamma_{12} Q_{12} + id_{21}E_{\mathrm{II}}^{(+)}(Q_{11} - Q_{22}) - id_{01}E_{\mathrm{I}}^{(-)} Q_{02} - id_{31}E_3^* Q_{32} + \mathcal{F}_{12},$$

$$\dot{Q}_{31} = -i\Gamma_{31} Q_{31} - id_{13}E_3(Q_{11} - Q_{33}) + id_{10}E_{\mathrm{I}}^{(+)} Q_{30} + id_{12}E_{\mathrm{II}}^{(-)} Q_{32} + \mathcal{F}_{31},$$

$$\dot{Q}_{02} = -i\Gamma_{02} Q_{02} + id_{21}E_{\mathrm{II}}^{(+)} Q_{01} - id_{10}E_{\mathrm{I}}^{(+)} Q_{12} + \mathcal{F}_{02},$$

$$\dot{Q}_{03} = -i\Gamma_{03} Q_{03} + id_{31}E_3^* Q_{01} - id_{10}E_{\mathrm{I}}^{(+)} Q_{13} + \mathcal{F}_{03},$$

$$\dot{Q}_{32} = -i\Gamma_{32} Q_{32} - id_{13}E_3 Q_{12} + id_{21}E_{\mathrm{II}}^{(+)} Q_{31} + \mathcal{F}_{32}. \tag{4}$$

In Eq. (4), γ_j $(j=0-3)$ are decay rates for each level and complex detunings are defined as $\Gamma_{01}=\Delta_1-i\gamma_{01}$, $\Gamma_{12}=\Delta_2-i\gamma_{12}$, $\Gamma_{31}=\Delta_3-i\gamma_{31}$, $\Gamma_{02}=\Delta_1+\Delta_2-i\gamma_{02}$, $\Gamma_{03}=\Delta_1-\Delta_3-i\gamma_{03}$, and $\Gamma_{32}=\Delta_2+\Delta_3-i\gamma_{32}$, respectively, where γ_{mn} $(m\neq n)$ are dephasing rates. To describe the atomic and field fluctuations, we have introduced the quantum Langevin noise operators $\mathcal{F}_{ij}$ $(i,j=0-3)$ into Eq. (4). In the two-photon limit, the Langevin noise operators introduce the unpaired photons which are not of interest here and we will ignore them from now on [26]. Without considering the generated fields and the input ω_2 beam, Eq. (4) reduces to a set of equations which describe the atomic dynamics of a standard three-level Λ-type EIT system, as expected. If the addressing field ω_3 is blocked and the produced fields are neglected, Eq. (4) describes the atomic evolution of a ladder-type EIT system [27]. The coexistence of these two EIT distinguishes the inverted-Y scheme from the double-Λ configuration [3,4,8,10–12], where only one Λ-type EIT is presented in the system. We now consider the details of the inverted-Y system.

Equation (4) includes the optical saturation effect and generally cannot be solved exactly. As described by Eq. (4), the atomic operators oscillate at an infinite number of frequencies. We are interested in the situation where ω_2 and ω_3 pump fields are treated correctly to all orders, while E_1, E_a, and E_b are kept to the lowest order only. Then the polarization will oscillate at four dominant frequencies ω_1, ω_2, $\omega_1+\delta$, and $\omega_2-\delta$. By extending the treatment introduced in [10,14,23,24], the steady-state solutions of Eq. (4) are required to be of the form

$$Q_{mn}=a_{mn}+b_{mn}e^{-i\delta t}+c_{mn}e^{i\delta t}\quad (m,n=0-3), \tag{5}$$

where a_{mn} are the solutions for the case in which only input fields are considered and b_{mn} and c_{mn} are assumed to be small such that $|b_{mn}|,|c_{mn}|\ll|a_{mn}|$. Since all the population is assumed to be mainly in the ground level $|0\rangle$, we choose $a_{00}\approx 1$. Next, we substitute the trial solution (5) into Eq. (4) and look at the terms with the same time dependence. We linearize the equations in E_a, E_b, and E_1 and obtain

$$a_{01}=\frac{4d_{10}\Gamma_{02}\Gamma_{03}E_1}{\mathcal{D}(0)},\quad a_{12}=-\frac{|\Omega_1|^2d_{21}E_2}{\mathcal{D}(0)}, \tag{6}$$

$$b_{01}=\frac{4d_{10}(\Gamma_{02}-\delta)(\Gamma_{03}-\delta)E_a^{(+)}}{\mathcal{D}_1(-\delta)}+\frac{16d_{21}E_2d_{10}E_1d_{12}\Gamma_{03}(\Gamma_{02}-\delta)(\Gamma_{03}-\delta)E_b^{(-)}}{\mathcal{D}(0)\mathcal{D}_1(-\delta)}, \tag{7}$$

$$c_{12}=-\frac{|\Omega_1|^2d_{21}\Gamma_{02}\Gamma_{03}E_b^{(+)}}{(\Gamma_{12}+\delta)(\Gamma_{02}+\delta)\mathcal{D}(0)}-\frac{4d_{10}E_1d_{21}E_2d_{01}\Gamma_{03}E_a^{(-)}}{(\Gamma_{12}+\delta)\mathcal{D}(0)}, \tag{8}$$

where

$$\mathcal{D}(0)=4\Gamma_{01}\Gamma_{02}\Gamma_{03}-\Gamma_{03}|\Omega_2|^2-\Gamma_{02}|\Omega_3|^2,$$

$$\mathcal{D}_1(-\delta)=4(\Gamma_{01}-\delta)(\Gamma_{02}-\delta)(\Gamma_{03}-\delta)-(\Gamma_{03}-\delta)|\Omega_2|^2-(\Gamma_{02}-\delta)|\Omega_3|^2. \tag{9}$$

In Eqs. (6)–(9), we define $\Omega_1=2d_{10}E_1$ as the weak pump Rabi frequency, $\Omega_2=2d_{21}E_2$ as the strong pump Rabi frequency, and $\Omega_3=2d_{13}E_3$ as the dressing laser Rabi frequency. Since the population is assumed to be in the ground state $|0\rangle$, we have simplified expressions (6)–(8) by taking $|\Gamma_{02}\Gamma_{12}|\gg|\Omega_1|^2$. This approximation is readily achieved by assuming the weak pump beam E_1 far off resonance $|0\rangle\rightarrow|1\rangle$ or $\gamma_{02}\gamma_{12}\gg|\Omega_1|^2$. The physics of Eqs. (6)–(8) can be understood as follows. Equation (6) describes the optical responses of the medium to two input pump fields E_1 and E_2, and the EIT signature appears in the E_1 channel. As expected, the E_1 field may be controlled by two sets of EIT. Equations (7) and (8) are related with the optical responses to the generated ω_a and ω_b fields, respectively. As we shall see, these contribute to the linear susceptibilities and the third-order nonlinear susceptibilities.

We are interested in the optical response of the atomic dipoles oscillating at frequencies $\omega_1+\delta$ and $\omega_2-\delta$. In the slowly varying amplitude approximation, polarization operators are given by $\mathcal{P}_a(\delta)=N\hbar d_{01}b_{01}$ and $\mathcal{P}_b(-\delta)=N\hbar d_{12}c_{12}$ for the atomic density N. The relationship between the polarization and the fields is $\mathcal{P}=\epsilon_0\chi E+\epsilon_0\chi^{(3)}EEE$, where χ is the linear susceptibility and $\chi^{(3)}$ is the third-order nonlinear susceptibility [23]. Using Eqs. (7)–(9), the linear and third-order nonlinear susceptibilities are

$$\chi_a(\delta)=\frac{4N\hbar|d_{10}|^2(\Gamma_{02}-\delta)(\Gamma_{03}-\delta)}{\epsilon_0\mathcal{D}_1(-\delta)}, \tag{10}$$

$$\chi_b(-\delta)=-\frac{N\hbar|\Omega_1|^2|d_{21}|^2\Gamma_{02}\Gamma_{03}}{\epsilon_0(\Gamma_{12}+\delta)(\Gamma_{02}+\delta)\mathcal{D}(0)}, \tag{11}$$

$$\chi_a^{(3)}(\delta)=\frac{16N\hbar|d_{10}d_{21}|^2\Gamma_{03}(\Gamma_{02}-\delta)(\Gamma_{03}-\delta)}{\epsilon_0\mathcal{D}(0)\mathcal{D}_1(-\delta)}, \tag{12}$$

$$\chi_b^{(3)}(-\delta)=-\frac{4N\hbar|d_{10}d_{21}|^2\Gamma_{03}}{\epsilon_0(\Gamma_{12}+\delta)\mathcal{D}(0)}. \tag{13}$$

The linear susceptibilities $\chi_a(\delta)$ and $\chi_b(-\delta)$ control the dispersion profile and transmission spectrum of the generated ω_a and ω_b fields as they propagate through the medium. As a consequence, these linear susceptibilities will govern the natural spectral width of paired photons through the phase matching condition. Again, as described in Eq. (10), two sets of EIT may exist in the generated ω_a channel. One is the ladder-type EIT due to the strong input E_2 beam and the other is the standard Λ-type EIT due to the dressing laser E_3. The parametric conversion efficiency of twin beams is governed by the third-order nonlinear susceptibilities $\chi_a^{(3)}(\delta)$ and $\chi_b^{(3)}(-\delta)$. The structure of these nonlinearities plays an important role in determining the feature of the two-photon amplitude (or biphoton wave packet) and will be evaluated in Sec. III B. Comparing with the two-photon cascade emission discussed in [21], Eqs. (12) and (13) not only recover the physics presented in [21], but also show the complicated

polarizability to the ω_a field because of the dressing laser, E_3. The linewidths in $\chi_a^{(3)}$ and $\chi_b^{(3)}$ set a limitation for the coherence time of paired photons. It should be noted that due to the presence of the denominator $\mathcal{D}(0)$ shown in $\chi_a^{(3)}(\delta)$, the parametric conversion efficiency is reduced. This indicates how to enhance the SWM process by suppressing the FWM in such an inverted-Y system, as experimentally demonstrated in [17–19].

To get further physical insights into Eqs. (12) and (13), it is helpful to look at the resonant feature of the quantity $\mathcal{D}_1(-\delta)$ defined in Eq. (9). The exact roots of the real part of $\mathcal{D}_1(-\delta)$ are very complicated. Instead of looking at these exact solutions, we focus on two simple cases in which (a) $\mathcal{D}_1(-\delta)\approx(\Gamma_{02}-\delta)[4(\Gamma_{01}-\delta)(\Gamma_{03}-\delta)-|\Omega_3|^2]$ with $|\Omega_3|\gg|\Omega_2|$ and (b) $\mathcal{D}_1(-\delta)\approx(\Gamma_{03}-\delta)[4(\Gamma_{01}-\delta)(\Gamma_{02}-\delta)-|\Omega_2|^2]$ with $|\Omega_3|\ll|\Omega_2|$. For case (a), utilizing Eq. (12) there are two resonances which occur at

$$\delta_{\pm}^{(a)}=\Delta_1-\frac{\Delta_3}{2}\pm\sqrt{\frac{|\Omega_3|^2}{4}+\frac{\Delta_3^2}{4}+\gamma_{01}\gamma_{03}}, \tag{14}$$

with the associated linewidths

$$\Gamma_{\pm}^{(a)}=\frac{\gamma_{01}+\gamma_{03}}{2}\pm\frac{\Delta_3(\gamma_{01}-\gamma_{03})}{2\sqrt{|\Omega_3|^2+\Delta_3^2+4\gamma_{01}\gamma_{03}}}. \tag{15}$$

These two resonances correspond to two FWM processes existing in the system. The generated ω_a field is centered at $\omega_1+\delta_{\pm}^{(a)}$, and the ω_b field is then centered at $\omega_2-\delta_{\pm}^{(a)}$. The frequency difference between two resonances for the ω_a (or ω_b) photons is $\sqrt{|\Omega_3|^2+\Delta_3^2+4\gamma_{01}\gamma_{03}}$. If the dressing laser E_3 is near resonant with the transition $|3\rangle\rightarrow|1\rangle$, the generated ω_a and ω_b beams are peaking at $\omega_{10}\pm\sqrt{|\Omega_3|^2+4\gamma_{01}\gamma_{03}}/2$ and $\omega_1+\omega_2-\omega_{10}\mp\sqrt{|\Omega_3|^2+4\gamma_{01}\gamma_{03}}/2$, respectively, and the associated linewidths equal the same value, $(\gamma_{01}+\gamma_{03})/2$. If the atomic coherence between $|0\rangle$ and $|3\rangle$ is long lived, $\Gamma_{\pm}^{(a)}$ is approximately determined by the dephasing rate between the transition $|0\rangle\rightarrow|1\rangle$, $\gamma_{01}/2$. In paired-photon generation, these two types of FWMs will interfere with each other if the detectors cannot spectrally resolve them. If the Rabi frequency of the dressing beam is large enough, two resonances will be well separated.

For case (b), using Eq. (13) the reduced two resonances appear at

$$\delta_{\pm}^{(b)}=\Delta_1+\frac{\Delta_2}{2}\pm\sqrt{\frac{|\Omega_2|^2}{4}+\frac{\Delta_2^2}{4}+\gamma_{01}\gamma_{02}} \tag{16}$$

and the associated linewidths are

$$\Gamma_{\pm}^{(b)}=\frac{\gamma_{01}+\gamma_{02}}{2}\pm\frac{\Delta_2(\gamma_{01}-\gamma_{02})}{2\sqrt{|\Omega_2|^2+\Delta_2^2+4\gamma_{01}\gamma_{02}}}. \tag{17}$$

From Eq. (16) we know that the generated ω_a field is resonant at $\omega_1+\delta_{\pm}^{(b)}$. The ω_b beam is then resonant at $\omega_2-\delta_{\pm}^{(b)}$. To eliminate the absorption of the ω_b photons, one can detune the strong pump beam E_2 far off the resonance with the transition $|1\rangle\rightarrow|2\rangle$. The frequency difference between these two resonances for the ω_a (or ω_b) photons becomes $\sqrt{|\Omega_2|^2+\Delta_2^2+4\gamma_{01}\gamma_{02}}$. As in case (a), the two FWM processes may interfere with each other. It is interesting to notice that the above analysis has a direct connection with that in the dressed-state picture. To simplify the discussion, in the following we take case (a) as the example to analyze the paired-photon generation in detail. In this example, we will assume that the dressing laser E_3 is near resonant with its atomic transition and the E_2 field is far off resonance.

Before proceeding the discussion, it is necessary to look at the phase-matching condition in such a cascade configuration. The propagation constants of two generated weak fields within the medium are given by $k_a=(\varpi_a+\delta)/v_a$ and $k_b=(\varpi_b-\delta)/v_b$, respectively, where $\varpi_{a,b}$ are the central frequency of the a and b fields and v_a and v_b are their group velocities in the atomic ensemble. Only when the dressing laser is (near) resonant—i.e., $\Delta_3\approx 0$—will the group velocity of the a field be dramatically changed due to the EIT slow-light effect. Otherwise, its group velocity can be set as the speed of light in vacuum, c. For the ω_b field, its group velocity approaches c because $|\Omega_2/\Gamma_{02}|\ll 1$. The group velocity of the a field can be evaluated by following the calculations shown in [10]. In the counterpropagating geometry, the resulting wave-number mismatch is

$$\Delta k=k_1-k_2+k_b-k_a=-\left(\frac{1}{c}+\frac{1}{v_a}\right)\delta+\frac{\omega_1}{v_1}-\frac{\varpi_a}{c}-\frac{\omega_2-\varpi_b}{c}, \tag{18}$$

where v_1 is the group velocity of the input ω_1 beam. On the other hand, the propagations of the a and b fields are limited by the transmission spectrums determined by the imaginary parts of their linear susceptibilities χ_a and χ_b, especially for the a beam. In the photon joint measurement, only if the ω_a photon is detected may one ensure that its twin is produced in the process. Therefore, we will use $\chi_a^{(3)}(\delta)$ to calculate the two-photon wave packet. Moreover, in order to ensure the ω_a photons entangled with the ω_b photons, γ_{01} should be much larger than γ_{12} so that the paired photons are temporally indistinguishable. Furthermore, we will assume that the linewidth of the generated ω_a field remains in the EIT bandwidth. In other words, we are interested in the biphoton bandwidth which is mainly determined by the linewidths instead of the phase dispersion or the transmission profiles. The statement will be further explained in Sec. III B.

B. Paired Stokes–anti-Stokes generator with EIT assistance

Generating paired Stokes and anti-Stokes photons has been experimentally demonstrated in the double-Λ schemes by Harris' group [3,4] in rubidium gas, where the EIT assists the propagation of the anti-Stokes field. In this section, we will examine the paired Stokes–anti-Stokes generation in a dressed four-level inverted-Y system [see Fig. 1(c)]. Comparing with the previous double-Λ schemes [3,4], the EIT effects offered in the current configuration [Fig. 1(c)] may be manipulated by altering either the Rabi frequency of the control laser or the Rabi frequency of the dressing beam, or both.

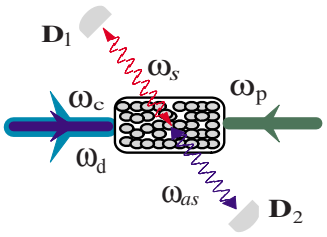

FIG. 2. (Color online) Backward detection geometry for paired Stokes and anti-Stokes photons generation.

As shown in Fig. 1(c), the weak probe beam with angular frequency ω_p and the strong control field with angular frequency ω_c are counterpropagating through the ensemble. Paired Stokes and anti-Stokes photons are spontaneously emitted into opposite directions. The weak probe field (ω_p) is (near resonantly) tuned to the atomic transition $|0\rangle \rightarrow |1\rangle$ with detuning $\Delta_p = \omega_{10} - \omega_p$, and the strong control beam is (near) resonant to the transition $|3\rangle \rightarrow |1\rangle$ with detuning $\Delta_c = \omega_{13} - \omega_c$. A dressing laser with angular frequency ω_d is applied to the transition $|1\rangle \rightarrow |2\rangle$ with detuning $\Delta_d = \omega_{21} - \omega_d$. The generated Stokes and anti-Stokes photons are centered around $\varpi_s = \omega_{13} - \Delta_p$ and $\varpi_{as} = \omega_{10} - \Delta_c$, respectively. The two-photon detunings are defined as $\Delta_{03} = \Delta_p - \Delta_c$, $\Delta_{02} = \Delta_p + \Delta_d$, and $\Delta_{32} = \Delta_c + \Delta_d$. Due to the strong intensities of the control and dressing lasers, perturbation theory is not sufficient to characterize the interaction between the medium and the input fields. We therefore will choose the same methodology introduced in [10,14,23,24] to analyze the atomic dynamics for the current configuration. In the proposed experimental setup, the backward detection geometry is chosen for the two detectors D_1 and D_2; see Fig. 2. The spatial positions of two detectors depends on the phase matching achieved in the experiment. For instance, if $\vec{k}_p + \vec{p}_c = 0$ is well satisfied, the right-angle geometry can be chosen for placing the detectors. It is assumed that the Stokes photons trigger detector D_1 and the anti-Stokes photons fire detector D_2.

We write the positive-frequency field operators as follows:

$$E_{\mathrm{I}}^{(+)} e^{-i\omega_p t} = [E_p + E_{as}^{(+)} e^{-i(\Delta_{03}+\delta)t}] e^{-i\omega_p t},$$

$$E_{\mathrm{II}}^{(+)} e^{-i\omega_c t} = [E_c + E_s^{(+)} e^{i(\Delta_{03}+\delta)t}] e^{-i\omega_c t}, \tag{19}$$

and the dressing laser E_d is treated as a classical field. To eliminate fast oscillating terms in Eq. (1), we introduce the following transformations:

$$Q_{ii} = \sigma_{ii} \quad (i = 0,1,2,3),$$

$$Q_{01} = \sigma_{01} e^{i\omega_p t}, \quad Q_{12} = \sigma_{12} e^{i\omega_d t}, \quad Q_{31} = \sigma_{31} e^{i\omega_c t},$$

$$Q_{02} = \sigma_{02} e^{i(\omega_p + \omega_d)t}, \quad Q_{03} = \sigma_{03} e^{i(\omega_p - \omega_c)t}, \quad Q_{32} = \sigma_{32} e^{i(\omega_c + \omega_d)t}. \tag{20}$$

By substituting Eqs. (19) and (20) into (1), in the rotating-wave approximation the set of equations of motion becomes

$$\dot{Q}_{00} = -\gamma_0 Q_{00} + i d_{01} E_{\mathrm{I}}^{(-)} Q_{01} - i d_{10} E_{\mathrm{I}}^{(+)} Q_{10} + \mathcal{F}_{00},$$

$$\dot{Q}_{11} = -\gamma_1 Q_{11} + i d_{10} E_{\mathrm{I}}^{(+)} Q_{10} - i d_{01} E_{\mathrm{I}}^{(-)} Q_{01} + i d_{12} E_d^* Q_{12} - i d_{21} E_d Q_{21} + i d_{13} E_{\mathrm{II}}^{(+)} Q_{13} - i d_{31} E_{\mathrm{II}}^{(-)} Q_{31} + \mathcal{F}_{11},$$

$$\dot{Q}_{22} = -\gamma_2 Q_{22} + i d_{21} E_d Q_{21} - i d_{12} E_d^* Q_{12} + \mathcal{F}_{22},$$

$$\dot{Q}_{33} = -\gamma_3 Q_{33} + i d_{31} E_{\mathrm{II}}^{(-)} Q_{31} - i d_{13} E_{\mathrm{II}}^{(+)} Q_{13} + \mathcal{F}_{33},$$

$$\dot{Q}_{01} = -i\Gamma_{01} Q_{01} + i d_{10} E_{\mathrm{I}}^{(+)} (Q_{00} - Q_{11}) + i d_{12} E_d^* Q_{02} + i d_{13} E_{\mathrm{II}}^{(+)} Q_{03} + \mathcal{F}_{01},$$

$$\dot{Q}_{12} = -i\Gamma_{12} Q_{12} + i d_{21} E_d (Q_{11} - Q_{22}) - i d_{01} E_{\mathrm{I}}^{(-)} Q_{02} - i d_{31} E_{\mathrm{II}}^{(-)} Q_{32} + \mathcal{F}_{12},$$

$$\dot{Q}_{31} = -i\Gamma_{31} Q_{31} - i d_{13} E_{\mathrm{II}}^{(+)} (Q_{11} - Q_{33}) + i d_{10} E_{\mathrm{I}}^{(+)} Q_{30} + i d_{12} E_d^* Q_{32} + \mathcal{F}_{31},$$

$$\dot{Q}_{02} = -i\Gamma_{02} Q_{02} + i d_{21} E_d Q_{01} - i d_{10} E_{\mathrm{I}}^{(+)} Q_{12} + \mathcal{F}_{02},$$

$$\dot{Q}_{03} = -i\Gamma_{03} Q_{03} + i d_{31} E_{\mathrm{II}}^{(-)} Q_{01} - i d_{10} E_{\mathrm{I}}^{(+)} Q_{13} + \mathcal{F}_{03},$$

$$\dot{Q}_{32} = -i\Gamma_{32} Q_{32} - i d_{13} E_{\mathrm{II}}^{(+)} Q_{12} + i d_{21} E_d Q_{31} + \mathcal{F}_{32}. \tag{21}$$

Again, as stated in Sec. II A, the Langevin noise operators in Eq. (21) will be neglected in the two-photon limit. One may notice that two types of EIT exist in the system for the input probe beam, a ladder-type and a Λ-type, as shall be formally shown below.

Equation (21) generally cannot be solved exactly for the fields given in Eq. (19). Instead we are interested in a situation where the control and dressing fields are treated to all orders, but the probe, Stokes, and anti-Stokes fields are kept to the lowest order only. The atomic response of interest will oscillate at four dominant frequencies ω_p, ω_c, $\omega_{10} + \delta$, and $\omega_{13} - \Delta_p - \delta$. Therefore, the steady-state solutions of Eq. (21) are required to take the form [10]

$$Q_{mn} = A_{mn} + B_{mn} e^{-i(\Delta_{03}+\delta)t} + C_{mn} e^{i(\Delta_{03}+\delta)t} \quad (m,n = 0-3), \tag{22}$$

where A_{mn} are the solutions for the case in which only input fields are considered and B_{mn} and C_{mn} are assumed to be small so that $|B_{mn}|, |C_{mn}| \ll |A_{mn}|$. For simplicity, all the population is assumed to be mainly located at the ground state $|0\rangle$ such that $A_{00} \approx 1$. Next, we plug the trial solution (22) into Eq. (21) and look at the terms with the same time dependence. Any term contains the product of more than one small quantity will be dropped. After some algebra, under the linearization procedure one can obtain the following quantities of interest:

$$A_{01} = \frac{4d_{10}\Gamma_{02}\Gamma_{03}E_p}{\mathcal{D}(0)}, \quad A_{31} = \frac{|\Omega_p|^2 d_{13}\Gamma_{02}^* E_c}{\Gamma_{13}^* \mathcal{D}^*(0)}, \tag{23}$$

$$B_{01} = \frac{4d_{10}(\Gamma_{02} - \Delta_{03} - \delta)(\Gamma_{03} - \Delta_{03} - \delta)E_{as}^{(+)}}{\mathcal{D}_2(-\Delta_{03} - \delta)} + \frac{16d_{10}E_p d_{13}E_c d_{31}\Gamma_{02}\Gamma_{03}(\Gamma_{02} - \Delta_{03} - \delta)E_s^{(-)}}{\mathcal{D}(0)\mathcal{D}_2(-\Delta_{03} - \delta)}, \tag{24}$$

$$C_{31} = \frac{|\Omega_p|^2 d_{13}\Gamma_{02}^*\Gamma_{03}^*[4(\Gamma_{01}^* - \Delta_{03} - \delta)(\Gamma_{02}^* - \Delta_{03} - \delta) - |\Omega_d|^2]E_s^{(+)}}{(\Gamma_{13}^* + \Delta_{03} + \delta)\mathcal{D}^*(0)\mathcal{D}_2^*(-\Delta_{03} - \delta)} + \frac{4d_{10}E_p d_{13}E_c d_{01}(\Gamma_{02}^* - \Delta_{03} - \delta)E_{as}^{(-)}}{(\Gamma_{13}^* + \Delta_{03} + \delta)\mathcal{D}_2^*(-\Delta_{03} - \delta)}, \tag{25}$$

where

$$\mathcal{D}_2(-\Delta_{03} - \delta) = 4(\Gamma_{01} - \Delta_{03} - \delta)(\Gamma_{02} - \Delta_{03} - \delta)(\Gamma_{03} - \Delta_{03} - \delta) - (\Gamma_{03} - \Delta_{03} - \delta)|\Omega_d|^2 - (\Gamma_{02} - \Delta_{03} - \delta)|\Omega_c|^2 \tag{26}$$

and $\mathcal{D}(0)$ is given in Eq. (9) except that $\Omega_{1,2,3}$ have been replaced by $\Omega_{p,d,c}$. In Eqs. (23)–(26), Ω_p, Ω_c, and Ω_d are the Rabi frequencies of the probe, control, and dressing beams, respectively. As expected, Eqs. (23)–(26) have recovered the results obtained in [10] for a three-level double-Λ configuration. The propagation constants of the probe and the control fields are determined by Eq. (23). It is now clear that two sets of EIT effects may coexist in the probe channel as mentioned previously. The linear and nonlinear optical responses of the atomic ensemble to the anti-Stokes and Stokes fields rely on Eqs. (24) and (25).

The slowly varying amplitudes of polarization operators for such a medium are given by $\mathcal{P}_s(-\delta) = N\hbar d_{31}C_{31}$ and $\mathcal{P}_{as}(\delta) = N\hbar d_{01}B_{01}$. By using the relationship between the polarization and the fields, $\mathcal{P} = \epsilon_0\chi E + \epsilon_0\chi^{(3)}EEE$, it is ready to find that the linear susceptibilities and the third-order nonlinear susceptibilities of the Stokes and anti-Stokes fields are

$$\chi_s(-\delta) = \frac{N\hbar|\Omega_p|^2|d_{13}|^2\Gamma_{02}^*\Gamma_{03}^*[4(\Gamma_{01}^* - \Delta_{03} - \delta)(\Gamma_{02}^* - \Delta_{03} - \delta) - |\Omega_d|^2]}{\epsilon_0\mathcal{D}^*(0)(\Gamma_{13}^* + \Delta_{03} + \delta)\mathcal{D}_2^*(-\Delta_{03} - \delta)}, \tag{27}$$

$$\chi_{as}(\delta) = \frac{4N\hbar|d_{10}|^2(\Gamma_{02} - \Delta_{03} - \delta)(\Gamma_{03} - \Delta_{03} - \delta)}{\epsilon_0\mathcal{D}_2(-\Delta_{03} - \delta)}, \tag{28}$$

$$\chi_s^{(3)}(-\delta) = \frac{4N\hbar|d_{10}d_{13}|^2(\Gamma_{02}^* - \Delta_{03} - \delta)}{\epsilon_0(\Gamma_{13}^* + \Delta_{03} + \delta)\mathcal{D}_2^*(-\Delta_{03} - \delta)}, \tag{29}$$

$$\chi_{as}^{(3)}(\delta) = \frac{16N\hbar|d_{10}d_{13}|^2\Gamma_{02}\Gamma_{03}(\Gamma_{02} - \Delta_{03} - \delta)}{\epsilon_0\mathcal{D}(0)\mathcal{D}_2(-\Delta_{03} - \delta)}. \tag{30}$$

The physics of Eqs. (27)–(30) has already been explored in the previous literature [8,10,14,15], and we will not repeat here. Instead, we are interested in the resonance structure determined by the quantity $\mathcal{D}_2(-\Delta_{03} - \delta)$ in Eq. (26). The reason is that the resonances shown in $\mathcal{D}_2(-\Delta_{03} - \delta)$ will tell the generation mechanisms behind the FWM processes—e.g., how many modes can be generated for the Stokes and anti-Stokes fields and how these modes are correlated with each other. Solving the cubic function $\mathrm{Re}[\mathcal{D}_2(-\Delta_{03} - \delta)] = 0$, where $\mathrm{Re}[x]$ means choosing the real part of the quantity x, one can find three roots which indicate a triplet of resonances. Alternatively, there are three types of FWM processes occurring in the interaction. Since these three roots take very complicated forms, in the following we look at two simple cases by using the similar arguments for the dressed cascade scheme in Sec. II A. Further, to satisfy almost of the population remaining in the ground state $|0\rangle$, we assume that the weak probe beam is far off resonant with the atomic transition $|0\rangle \rightarrow |1\rangle$. Under such an assumption, the expressions of $\chi_s^{(3)}(-\delta)$ and $\chi_{as}^{(3)}(\delta)$ share the symmetry. One simple case is that we approximate $\mathcal{D}_2(-\Delta_{03} - \delta)$ as $(\Gamma_{02} - \Delta_{03} - \delta) \times [4(\Gamma_{01} - \Delta_{03} - \delta)(\Gamma_{03} - \Delta_{03} - \delta) - |\Omega_c|^2]$. Combining with Eq. (30), one may realize that the system is reduced to the three-level double-Λ case as discussed in [10]. The analysis applied in [10] can be easily extended to the current situation. Hence, we will skip this case and interested readers may resort to Ref. [10] for details. The other case is that $\mathcal{D}_2(-\Delta_{03} - \delta)$ may be approximated as $(\Gamma_{03} - \Delta_{03} - \delta)[4(\Gamma_{01} - \Delta_{03} - \delta)(\Gamma_{02} - \Delta_{03} - \delta) - |\Omega_d|^2]$. In this latter case, the EIT effect mainly comes from the strong dressing field E_d not from the control laser E_c. To see the optical responses of the

medium to the generated Stokes and anti-Stokes fields in such a case, we rewrite Eqs. (27)–(30) as

$$\chi_s(-\delta) = -\frac{N\hbar\Gamma_{02}^*|\Omega_p|^2|d_{13}|^2}{\epsilon_0(4\Gamma_{01}^*\Gamma_{02}^* - |\Omega_d|^2)(\Delta_p + \delta + i\gamma_{13})(\delta - i\gamma_{03})}, \tag{31}$$

$$\chi_{as}(\delta) = \frac{4N\hbar|d_{10}|^2(\Delta_{32} - \delta - i\gamma_{02})(\delta + i\gamma_{03})}{\epsilon_0\mathcal{D}_2(\delta)}, \tag{32}$$

$$\chi_s^{(3)}(-\delta) = -\frac{4N\hbar|d_{10}d_{13}|^2(\Delta_{32} - \delta + i\gamma_{02})}{\epsilon_0(\Delta_p + \delta + i\gamma_{13})\mathcal{D}_2^*(\delta)}, \tag{33}$$

$$\chi_{as}^{(3)}(\delta) = -\frac{16N\hbar|d_{10}d_{13}|^2\Gamma_{02}(\Delta_{32} - \delta - i\gamma_{02})}{\epsilon_0(4\Gamma_{01}\Gamma_{02} - |\Omega_d|^2)\mathcal{D}_2(\delta)}, \tag{34}$$

where

$$\mathcal{D}_2(\delta) = (\delta + i\gamma_{03})[4(\Delta_c - \delta - i\gamma_{01})(\Delta_{32} - \delta - i\gamma_{02}) - |\Omega_d|^2]. \tag{35}$$

From Eqs. (33) and (34), one may find that the nonlinearity to the Stokes field is slightly different from the nonlinearity to the anti-Stokes field. In the correlation measurement of paired Stokes-anti-Stokes photons, however, the triggering of an anti-Stokes photon will ensure its twin Stokes photon generated in the process, because after one cycle the population should return to the ground level $|0\rangle$. Hence, we will choose the anti-Stokes spectrum $[\chi_{as}^{(3)}(\delta)]$ to calculate the two-photon correlation. The linear response to the anti-Stokes field takes the EIT-like form while the response to the Stokes field is a Lorentzian line shape. Further, from Eq. (31) one may notice that if the central frequency of the generated Stokes photons coincides with the transition $|0\rangle \rightarrow |1\rangle$, they will be strongly absorbed and the absorption may weaken the assumption of $A_{00} \approx 1$. Fortunately, this absorption can be avoided because the FWM to produce Stokes photons in this mode is much weaker than other FWMs to create photons in other possible modes, as shown in Eq. (33).

The spectrum of the generated anti-Stokes field can be understood by examining the roots of the quantity $\mathcal{D}_2(\delta)$. By inspecting that the real part of $\mathcal{D}_2(\delta)$ vanishes, the triplet of resonances appears at

$$\delta_0 = 0, \quad \delta_\pm = \frac{2\Delta_c + \Delta_d \pm \sqrt{|\Omega_d|^2 + \Delta_d^2 + 4\gamma_{01}\gamma_{02}}}{2}. \tag{36}$$

In the limit of $\Delta_c \rightarrow 0$ and $\Delta_d \rightarrow 0$, $\delta_\pm$ approach to $\pm\sqrt{|\Omega_d|^2 + 4\gamma_{01}\gamma_{02}}/2$. To well separate these two modes, $|\Omega_d|$ is required to be greater than $\sqrt{\gamma_{01}\gamma_{02}}$ and this leads to $\delta_\pm \approx \pm|\Omega_d|/2$. The corresponding linewidths of the triplet of resonances [Eq. (36)] are

$$\Gamma_0 = \gamma_{03}, \quad \Gamma_\pm = \frac{\gamma_{01} + \gamma_{02}}{2} \pm \frac{\Delta_d(\gamma_{02} - \gamma_{01})}{2\sqrt{|\Omega_d|^2 + \Delta_d^2 + 4\gamma_{01}\gamma_{02}}}. \tag{37}$$

In the case of $\Delta_d \rightarrow 0$, $\Gamma_\pm$ both go to $(\gamma_{01} + \gamma_{02})/2$ while in the case of large dressing detuning ($|\Delta_d| \gg |\Omega_d|$), Γ_+ approaches γ_{02} and Γ_- goes to γ_{01}. Three types of FWMs appear behind $\mathcal{D}_2(\delta)$. One FWM process happens when the central frequency of the anti-Stokes field coincides with the atomic transition frequency, ω_{10}, and the central frequency of the Stokes field coincides with the atomic-transition frequency, $\omega_{13} - \Delta_p$. The second FWM occurs as the anti-Stokes field peaks at $\varpi_{as} = \omega_{10} - \Delta_c + \delta_+$ while the Stokes field peaks at $\varpi_s = \omega_{13} - \Delta_p - \delta_+$. The third FWM exists when the anti-Stokes mode is centered at $\omega_{10} - \Delta_c - \delta_-$ and the Stokes mode is centered at $\omega_{13} - \Delta_p - \delta_-$. As expected, all three FWMs satisfy the energy conservation $\omega_p + \omega_c - \varpi_s - \varpi_{as} = 0$. The linear optical response $\chi_s(-\delta)$ [Eq. (31)] to the Stokes field indicates that the generated mode centered at $\omega_{13} - \Delta_p$ will be strongly absorbed. As a consequence, this type of FWM will have a small compact on the two-photon coincidence counting measurement. The other two FWMs are far off with the absorption lines and will play the dominant role in determining the properties of the two-photon amplitude. The phase matching of the FWM processes in such a dressed double-Λ configuration can be analyzed by following the treatment introduced in [10] and we will not repeat the argument here. Instead, we will concentrate on the situation that the coherence time of paired Stokes–anti-Stokes photons is mainly determined by the linewidths of resonances instead of the phase matching (by manipulating the optical depth). The latter one may be used to generate paired photons with subnatural linewidth [13], which have potential applications in long-distance quantum communication and quantum information processing.

III. TWO-PHOTON TEMPORAL CORRELATION

A. Two-photon state

Following the procedure applied in [7,8,10], the two-photon state at the output surfaces of the medium reads [10]

$$|\Psi\rangle = \sum_{\vec{k}_a} \sum_{\vec{k}_b} F(\vec{k}_a, \vec{k}_b) a_{\vec{k}_a}^\dagger a_{\vec{k}_b}^\dagger |0\rangle. \tag{38}$$

$F(\vec{k}_a, \vec{k}_b)$ is the two-photon spectral function, and it takes the form

$$F(\vec{k}_a, \vec{k}_b) = \beta\delta(\delta_1 + \omega_2 - \omega_a - \omega_b)\Phi(\Delta kL)H_{tr}(\vec{\alpha}_a, \vec{\alpha}_b, \vec{\rho}). \tag{39}$$

In Eq. (39), the Dirac δ function comes from the time integral and physically it insists the energy conservation in the process. β is a constant which equals $i\pi\sqrt{\varpi_a\varpi_b}E_1E_2\chi_a^{(3)}$. $\Phi(\Delta kL)$ is the longitudinal detuning function, which is the z integral from $-L$ to 0 over the length of the ensemble,

$$\Phi(\Delta kL) = \mathrm{sinc}\left[\frac{\Delta kL}{2}\right] e^{-i\Delta kL/2}, \tag{40}$$

where $\Delta k = k_1 - k_c + k_b - k_a$ is the phase mismatching along with the longitudinal direction. $H_{tr}(\vec{\alpha}_a, \vec{\alpha}_b, \vec{\rho})$ is called the transverse detuning function, which is the integral over the area A of the intersection of the beam cross section:

$$H_{tr}(\vec{\alpha}_a, \vec{\alpha}_b, \vec{\rho}) = \frac{1}{A}\int_A d^2\rho\, e^{-i(\vec{\alpha}_a + \vec{\alpha}_b)\cdot\vec{\rho}}. \tag{41}$$

In the derivation of Eq. (41), A independent of z is assumed. $\vec{\alpha}_{a,b}$ are the transverse wave vectors of the generated correlated photons. $\vec{\rho}$ is sitting in the transverse plane perpendicular to the longitudinal axis z. It is obvious that Φ and H_{tr} both become δ functions in the limit of a medium with infinite length and cross-sectional area. Along with the energy conservation δ function, they together form perfect phase-matching conditions $\omega_1 + \omega_2 - \omega_a - \omega_b = 0$ and $\vec{k}_1 + \vec{k}_2 + \vec{k}_a + \vec{k}_b = \vec{0}$. On the one hand, the natural spectral width of the biphoton wave packet determined by Φ can be manipulated through changing the group delay between paired photons to traverse the medium. For example, in a dense atomic gas medium, using the EIT to alter the phase matching one can achieve the subnatural-linewidth photon pairs generation, where a coherence time close to 1 μs [13] is achievable. On the other hand, the transverse properties of entangled photons is governed by H_{tr}. The transverse correlation of entangled photons has practical applications in such as quantum imaging [28] and quantum lithography [29]. In this paper, we will focus on the temporal correlation. The transverse effects can be analyzed by following the procedures introduced in [8,30].

To simplify the proceeding discussions, we will assume that the intersection between the input beams is large enough so that the transverse detuning function H_{tr} is approximated as a δ function. The wave vectors will also be replaced by the wave numbers.

B. Correlation for cascade paired-photon emitter

To study the optical properties of paired photons produced from a dressed cascade system [Fig. 1(a)], we focus on a simple experiment of photon coincidence counting measurement, as illustrated in Fig. 1(d). It is assumed that the ω_a photons trigger the detector D_1 and the ω_b photons go to detector D_2. For simplicity, we will ignore the polarization properties of generated weak fields.

The averaged two-photon coincidence-counting rate is

$$R_c = \lim_{T\to\infty}\frac{1}{T}\int_0^T dt_1 \int_0^T dt_2 \langle\Psi|E_1^{(-)}(\tau_1)E_2^{(-)}(\tau_2)E_2^{(+)}(\tau_2)E_1^{(+)}(\tau_1) \times|\Psi\rangle S(\tau_1 - \tau_2), \tag{42}$$

where $|\Psi\rangle$ is given in Eq. (38), $E_j^{(+)}(\tau_j)$ $(j=1,2)$ are the free-space electromagnetic fields evaluated at detector D_j's spatial coordinate z_j and firing time t_j and $\tau_j = t_j - z_j/c$, respectively. $S(\tau_1 - \tau_2)$ is the coincidence-counting window function and it has the properties as $S=1$ for $|\tau_1 - \tau_2| < t_c$; otherwise, $S=0$. For the narrow-band biphoton generation discussed here, t_c is large enough so that one may set $S=1$. To further simplify the discussion, we have taken the detectors' efficiencies to be 100%. It should be noted that since we here are interested in narrow-band biphoton generation, the bandwidth of biphotons is smaller than the spectral width of the detectors used in the current laboratories. Therefore, the coincidence-counting rate (42) can be further simplified as

$$\begin{aligned} R_c &= \langle\Psi|E_1^{(-)}(\tau_1)E_2^{(-)}(\tau_2)E_2^{(+)}(\tau_2)E_1^{(+)}(\tau_1)|\Psi\rangle \\ &= |\langle 0|E_2^{(+)}(\tau_2)E_1^{(+)}(\tau_1)|\Psi\rangle|^2 \\ &= |A_c(\tau_1,\tau_2)|^2. \end{aligned} \tag{43}$$

$A_c(\tau)$ is usually referred to as the two-photon amplitude, or biphoton wave packet [7].

Without taking into account filters before the detectors, using Eq. (43) one thus obtains

$$A_c(\tau_1,\tau_2) = \sum_{\kappa_1}\sum_{\kappa_2} E_{\kappa_1}E_{\kappa_2}e^{-i(\nu_1\tau_1+\nu_2\tau_2)}\langle 0|a_{\kappa_2}a_{\kappa_1}|\Psi\rangle. \tag{44}$$

With the help of Eqs. (38) and (39), Eq. (44) can be further evaluated as

$$A_c(\tau_1,\tau_2) = \sum_{k_a}\sum_{k_b} A_{c0}\chi_a^{(3)}\delta(\omega_1+\omega_2-\omega_a-\omega_b) \times\Phi(\Delta kL)e^{-i(\omega_a\tau_1+\omega_b\tau_2)}, \tag{45}$$

where the slowly varying terms and constant are absorbed into A_{c0}. Next, we convert the sums in Eq. (45) into the angular-frequency integral. The two-photon amplitude (45) can be written as

$$A_c(\tau_+,\tau_-) = A_{c0}e^{-i(\omega_1+\omega_2)\tau_+/2}e^{-i(\varpi_a-\varpi_b)\tau_-/2} \times\int d\delta\,\chi_a^{(3)}(\delta)\mathrm{sinc}\left[\frac{\Delta kL}{2}\right]e^{i\delta[L(1/c+1/v_a)/2-\tau_-]}, \tag{46}$$

where Eqs. (18) and (40) have been used and all the slowly varying phase terms and constants are grouped into A_{c0}. In Eq. (46), we have also defined $\tau_+ = \tau_1 + \tau_2$ and $\tau_- = \tau_1 - \tau_2$. It is obvious from Eq. (46) that the two-photon amplitude is a convolution between the phase matching and the structure of the third-order nonlinearity. As mentioned in Sec. II A, in the following we focus on the case that the third-order nonlinearity plays a dominant role in determining the two-photon wave packet. So we will remove the longitudinal detuning function from Eq. (46) and write it as

$$A_c(\tau_+,\tau_-) = A_{c0}e^{-i(\omega_1+\omega_2)\tau_+/2}e^{-i(\varpi_a-\varpi_b)\tau_-/2}\int d\delta\,\chi_a^{(3)}(\delta)e^{-i\delta\tau_-}.$$

Clearly, the two-photon amplitude now turns to be the Fourier transform of $\chi_a^{(3)}(\delta)$. Because of the complexity of $\chi_a^{(3)}(\delta)$ [see Eq. (12)], we here only look at the case (a) as discussed in Sec. II A and formulate $\chi_a^{(3)}(\delta)$ as

$$\chi_a^{(3)}(\delta) = \frac{16N\hbar|d_{10}d_{21}|^2\Gamma_{03}}{\epsilon_0\mathcal{D}(0)} \frac{\Delta_1 - \Delta_3 - \delta - i\gamma_{03}}{(\delta - \delta_+^{(a)} + i\Gamma_+^{(a)})(\delta - \delta_-^{(a)} + i\Gamma_-^{(a)})}. \tag{47}$$

By substituting Eq. (47) into the above equation and keeping the majority quantities of interest, the biphoton wave packet now becomes

$$A_c(\tau_+, \tau_-) = A_{c0} e^{-i(\omega_1+\omega_2)\tau_+/2} e^{-i(\varpi_a - \varpi_b)\tau/2} \times \int d\delta \frac{(\Delta_1 - \Delta_3 - \delta - i\gamma_{03}) e^{-i\delta\tau}}{(\delta - \delta_+^{(a)} + i\Gamma_+^{(a)})(\delta - \delta_-^{(a)} + i\Gamma_-^{(a)})}, \tag{48}$$

where we have denoted τ_- as τ. Again, all the slowly varying terms and constants are absorbed into A_{c0}. By calculating the residues in Eq. (48), it gives

$$A_c(\tau_+, \tau) = A_{c0}\phi_c(\tau_+)\psi(\tau), \tag{49}$$

$$\phi_c(\tau_+) = e^{-i(\omega_1+\omega_2)\tau_+/2}, \tag{50}$$

$$\psi(\tau) = e^{-i(\varpi_a - \varpi_b)\tau/2}\left[e^{-i\delta_+^{(a)}\tau} e^{-\Gamma_+^{(a)}\tau} - e^{-i\delta_-^{(a)}\tau} e^{-\Gamma_-^{(a)}\tau}\right]. \tag{51}$$

The physics of Eq. (49) is understood as follows. Because the two-photon state is entangled, it cannot be factorized into a function of τ_1 times a function of τ_2. The function $\phi_c(\tau_+)$ describes that the pair is randomly created at any time within the ensemble. If taking into account the pulsed lasers, $\phi_c(\tau_+)$ would become a wave packet with coherence length of the E_1 and E_2 beams. The function $\psi(\tau)$ illustrates that in the two-photon amplitude, a destructive interference occurs between two FWMs shown in $\chi_a^{(3)}(\delta)$ (as previously mentioned in Sec. II A). The first term in the square brackets on the right-hand side of Eq. (51) represents the two-photon amplitude between correlated photons peaking at $\varpi_a = \omega_1 + \delta_+^{(a)}$ and $\varpi_b = \omega_2 - \delta_+^{(a)}$ with linewidth $\Gamma_+^{(a)}$; while the second term stands for the two-photon amplitude between paired photons centered at $\varpi_a = \omega_1 + \delta_-^{(a)}$ and $\varpi_b = \omega_2 - \delta_-^{(a)}$ with linewidth $\Gamma_-^{(a)}$. The sum of these two amplitudes is manifested by a slowly oscillating phase term. To further see this feature of $\psi(\tau)$, we look at one example in which the (near-)resonant dressing field assists the propagation of the generated ω_a fields through the EIT effect. To overlap the wave packets of the emitted ω_a and ω_b photons, γ_{01} is much larger than γ_{12} and γ_{03}. Hence, $\delta_\pm^{(a)} \approx \Delta_1 \pm |\Omega_3|/2$ and $\Gamma_\pm^{(a)} \approx \gamma_{01}/2$. Now $\psi(\tau)$ takes a simpler form

$$\psi(\tau) = e^{-i(\varpi_a - \varpi_b + 2\Delta_1)\tau/2} e^{-\gamma_{01}\tau/2} \sin\left(\frac{|\Omega_3|\tau}{2}\right). \tag{52}$$

It is clear that the two-photon amplitude will be a damped sinusoidal. This is different from the feature discussed in [21,22], where only an exponential decay curve appears. However, the physics is not difficult to understand. The strong dressing field changes the system states, especially the state $|1\rangle$, seeing by the generated ω_a and ω_b fields. If the detectors could spectrally distinguish these two FWMs, the two-photon amplitude will reduce to the result obtained in [21,22] and the interference will disappear. Another difference is that we have included the optical saturation in the susceptibilities.

By using Eq. (43) we find

$$R_c(\tau) = R_{c0}[1 - \cos(|\Omega_3|\tau)]e^{-\gamma_{01}\tau}, \tag{53}$$

where R_{c0} is a constant. Equation (53) shows that the two-photon interference pattern is a damped Rabi oscillation with the oscillation frequency given by the Rabi frequency of the dressing laser, $|\Omega_3|$. The damping rate is proportional to the dephasing rate γ_{01}. At $\tau=0$, R_c vanishes, indicating a photon anti-bunching-like effect. As $\tau \to \infty$, R_c again goes to zero. If $\vec{k}_1 + \vec{k}_2 = \vec{0}$, $R_c(\tau)$ would be a symmetric distribution about $\tau = 0$, since spontaneously emitted entangled photons can trigger both detectors D_1 and D_2.

C. Correlation for paired Stokes–anti-Stokes generator

Now we turn to the paired Stokes–anti-Stokes generation with EIT assistance in the inverted-Y system, shown in Fig. 1(c). The joint detection experimental setup is sketched in Fig. 2, where we assume that the Stokes photons go to detector D_1 and the anti-Stokes photons to detector D_2. The backward detection geometry will be considered in the following analysis. Again, the polarization properties of the generated weak fields will not be taken into account.

Using perturbation theory, in the two-photon limit the wave packet for paired Stokes and anti-Stokes photons takes the form [10]

$$A_r(\tau_+, \tau) = A_r e^{-i(\omega_p+\omega_c)\tau_+/2} e^{-i(\varpi_{as} - \varpi_s)\tau/2} \times \int d\delta\, \chi_{as}^{(3)}(\delta)\mathrm{sinc}\left[\frac{\Delta k_r L}{2}\right] e^{i\delta[L(1/c + 1/v_{as})/2 - \tau]}. \tag{54}$$

A_r contains all the slowly varying terms and constants. In Eq. (54), $\tau_+ = \tau_1 + \tau_2$ with $\tau_j = t_j - r_j/c$ $(j=1,2)$ and $\tau = \tau_1 - \tau_2$ is the space-time difference between clicks of two detectors. Δk_r is the wave-number mismatch. Similarly, the two-photon amplitude (54) is a convolution between the third-order nonlinearity $\chi_{as}^{(3)}(\delta)$ and the phase matching. As an example, we are going to look at optical properties of paired Stokes and anti-Stokes photons when $\chi_{as}^{(3)}(\delta)$ in (34) may be approximated as

$$\chi_{as}^{(3)}(\delta) = -\frac{4N\hbar|d_{10}d_{13}|^2\Gamma_{02}}{\epsilon_0(4\Gamma_{01}\Gamma_{02} - |\Omega_d|^2)} \times \frac{\Delta_{32} - \delta - i\gamma_{02}}{(\delta + i\gamma_{03})(\delta - \delta_+ + i\Gamma_+)(\delta - \delta_- + i\Gamma_-)}. \tag{55}$$

We are interested in the fact that the optical properties of the two-photon amplitude (54) are mainly determined by $\chi_{as}^{(3)}(\delta)$ not by the phase matching. In addition, the EIT effect comes from the strong dressing field E_d. Therefore, we will approximate $\Delta_d = 0$, $\Delta_c = 0$, and $|\Omega_d|^2 \gg \gamma_{01}\gamma_{02}$. Equation (54) now becomes

$$A_r(\tau_+,\tau) = A_r e^{-i(\omega_p+\omega_c)\tau_+/2} e^{-i(\varpi_{as}-\varpi_s)\tau/2} \int d\delta \frac{(\delta + i\gamma_{02}) e^{-i\delta\tau}}{(\delta + i\gamma_{03})[\delta - |\Omega_d|/2 + i(\gamma_{01}+\gamma_{02})/2][\delta + |\Omega_d|/2 + i(\gamma_{01}+\gamma_{02})/2]}. \quad (56)$$

Again, all the slowly varying terms and constants have been absorbed into A_r. The contour integral of Eq. (56) gives

$$A_r(\tau_+,\tau) = A_r \phi_r(\tau_+)\psi_r(\tau), \quad (57)$$

$$\phi_r(\tau_+) = e^{-i(\omega_p+\omega_c)\tau_+/2}, \quad (58)$$

$$\psi_r(\tau) = e^{-i(\varpi_{as}-\varpi_s)\tau/2}\left[\frac{\gamma_{02}-\gamma_{03}}{|\Omega_d|} e^{-\gamma_{03}\tau} - 4\sin\left(\frac{|\Omega_d|\tau}{2}\right) e^{-(\gamma_{01}+\gamma_{02})\tau/2}\right]. \quad (59)$$

Due to the triplet of resonances in $\chi_{as}^{(3)}(\delta)$, the two-photon amplitude is the sum of three FWMs. Because γ_{02} and $\gamma_{03} \ll |\Omega_d|$, Eq. (59) is reduced to a simple form

$$\psi_r(\tau) = e^{-i(\varpi_{as}-\varpi_s)\tau/2} \sin\left(\frac{|\Omega_d|\tau}{2}\right) e^{-(\gamma_{01}+\gamma_{02})\tau/2}. \quad (60)$$

This means that among three FWMs, the generated Stokes and anti-Stokes photons centered at $\varpi_s = \omega_{13}$ and $\varpi_{as} = \omega_{10}$ have a negligible contribution to the two-photon amplitude. Alternatively, the properties of biphoton wave packet for paired Stokes and anti-Stokes photons are mainly determined by the other two FWMs (peaking at $\varpi_s = \omega_{13} - \Delta_p - |\Omega_d|/2$, $\varpi_{as} = \omega_{10} + |\Omega_d|/2$ and $\varpi_s = \omega_{13} - \Delta_p + |\Omega_d|/2$, $\varpi_{as} = \omega_{10} - |\Omega_d|/2$).

By using Eqs. (57) and (43) with the help of Eqs. (58) and (60), the two-photon coincidence-counting rate reads

$$R_r(\tau) = R_r[1 - \cos(|\Omega_d|\tau)]e^{-(\gamma_{01}+\gamma_{02})\tau}, \quad (61)$$

where R_r is a constant. The physics is obvious: the destructive interference caused by two FWMs results in a damped Rabi oscillation in the two-photon joint detection probability. The oscillation period is equal to $2\pi/|\Omega_d|$ and the damping rate is equal to the resonant linewidths. As seen from Eq. (61), the two-photon coincidences go to zero at $\tau = 0$ and $\tau \to \infty$. This indicates that a photon anti-bunching-like effect appears in $R_r(\tau)$ due to the destructive interference between two FWMs. For instance, $R_r(0) = 0$ is resulted from such a destructive interference.

D. Comparison and discussion

Since two types of biphoton generations have been introduced in this paper, it is helpful to make some comparisons with previous paired-photon generation schemes.

First of all, let us compare the cascade two-photon emitter discussed in Sec. III B with the cases analyzed in [21,22]. One difference comes from the observed damped Rabi oscillations in two-photon coincidences. In the case of Ref. [21] it simply showed an exponential decay curvature in the two-photon temporal correlation. Ooi and Scully [22] extended the analysis of Ref. [21] and further showed that the Rabi oscillations will be obtained when considering the propagation of fields inside the atomic ensemble. Comparing these oscillations with the oscillations shown in Sec. III B, one may realize that the difference is due to the different physical mechanisms. The oscillations shown in Sec. III B are from the destructive interference between two types of FWM processes. Including the propagation properties of fields inside the medium, the two-photon coincidence counting rate will exhibit different behaviors depending on the optical depth, as pointed out in [9,10].

Second, the Rabi oscillation periods shown in the paired Stokes–anti-Stokes generator as discussed in Sec. III C and those presented in [3,4,8–12] are different. The case discussed in Sec. III C shows that the Rabi oscillation period can be a function of the dressing field intensity but not the control beam. The physics is due to which laser intensity is dominant in changing the dressed states seeing by the generated photons. One interesting question comes up when including the propagation properties of generated fields within the atomic ensemble. Certainly the curvature of the two-photon temporal correlation is a function of the optical depth. However, the competition between the Rabi oscillation and phase matching may result in unusual behavior, which is out of the scope of this paper.

It is known that in single-photon resonance fluorescence processes, one can find similar damped Rabi oscillations in the second-order correlation function. However, it is physically different from the Rabi oscillations observed in the case of paired-photon generation. In the single-photon fluorescence, the damped Rabi oscillations are understood as that once a photon has been emitted, it will take a time approximately equal to the Rabi transition before the next photon can be emitted [31]. This leads to the first observation of the photon anti-bunching effect. However, the Rabi oscillations observed in biphoton generation cases come from the destructive interference between two types of FWM processes, which also leads to the photon anti-bunching-like effect. These two oscillations can be distinguished theoretically and experimentally by looking at, e.g., the second-order quantum coherence function $g^{(2)}(\tau)$. In the single-photon fluorescence case, $g^{(2)}(0)$ is always smaller than $g^{(2)}(\infty)$; see, e.g., [31], while in the case of paired-photon generation, $g^{(2)}(0)$ [and $g^{(2)}(\infty)$] is close to 1, as experimentally demonstrated in [3–5].

Before ending this section, we notice several interesting issues about the four-level inverted-Y atomic system. For instance, by properly selecting the atomic transitions and choosing input laser intensities, it is possible to make the dressed ladder-type scheme and the dressed double-Λ-type configuration coexist in such a system. When reaching such a situation, one may not distinguish from which scheme paired

photons are generated. The two-photon amplitude would be the sum of all indistinguishable processes as required by quantum mechanics. As a consequence, the two-photon temporal correlation would be modulated differently, neither simply following each scheme. Moreover, because of the coexistence of the dressed ladder-type scheme and the dressed double-Λ-type configuration, there could be two or more photon pairs generated at the same time from the inverted-Y system. These multiple photon pairs might overlap their wave packets and therefore result in entangled three-photon or four-photon state production. Furthermore, six-wave mixing has been successfully demonstrated in the recent experiments by suppressing the FWM processes using the EIT effects [17–19]. This alternatively indicates that it is possible to create a three-photon state from the SWM process because the EIT will (sufficiently) suppress the weight of the two-photon state and enhance the conversion efficiency of SWM. This work will be done in the future.

IV. SUMMARY

In summary, we have studied the atomic dynamics in a four-level inverted-Y system. The feasibility of generating nonclassical light has been demonstrated by analyzing two possible configurations in the backward detection geometry. In the dressed cascade scheme, producing paired photons depends on the overlap of wave packets between twin photons, in agreement with the conclusion already presented in the literature [21,22]. However, since the dressing laser changes the states of the system seen by the weak fields, the damped Rabi oscillation can be observed in the two-photon coincidence counting measurement. This is in contrast with a simple exponential decay behavior exhibited in [21,22]. In the dressed paired Stokes–anti-Stokes generation with EIT assistance, we recover the results obtained in the three-level double-Λ configuration [4,10]. It is found that the two-photon temporal correlation can still behave as a damped Rabi oscillation. Further, this oscillation period can be manipulated by changing either the Rabi frequency of the control field or the Rabi frequency of the dressing laser, or both. The optical properties of the two-photon amplitude in each configuration are determined by the convolution between the phase matching and the third-order nonlinearity. For simplicity, we concentrate on the cases that the coherence time of paired photons is mainly determined by the resonant linewidths, not by the phase-matching condition. The observed damped Rabi oscillations in both schemes are due to the destructive interference among possible FWM processes occurring in the system. This destructive interference further leads to a photon anti-bunching-like effect in the two-photon coincidence counting measurement. Alternatively, the observed interference patterns can be thought of as two-photon beatings. If the detectors could spectrally distinguish each FWM modes, the interference will disappear and a simple exponential decay curve will be observed in the joint detection. It is possible for the dressed cascade scheme and the dressed double-Λ configuration to coexist in the inverted-Y system by properly selecting the atomic transitions and choosing the pump laser intensities. When approaching such a condition, the two-photon amplitude would be the sum of all the indistinguishable processes. The two-photon temporal correlation hence would be modulated differently, not just simply following the dynamics of each scheme.

The methodology adopted in this paper is proved to be a useful tool to study the optical spectroscopy in the atom-field interaction system. The theory further provides physical insights into the generation mechanism behind FWMs—e.g., how many modes could be created in the processes and how these modes are correlated with each other. For simplicity, the analysis presented here is not taken into account the Doppler effect, Langevin noise, and the polarization properties of generated fields.

ACKNOWLEDGMENTS

J.-M.W. and M.H.R. were supported in part by the (U.S.) Army Research Office under MURI Grant No. W911NF-05-1-0197. S.D. acknowledges financial support from the Defense Advanced Research Projects Agency, the (U.S.) Air Force Office of Scientific Research, and the (U.S.) Army Research Office. Y.P.Z. and M.X. were supported by the National Science Foundation.

[1] S. E. Harris, Phys. Today **50** (7), 36 (1997); M. Fleischhauer, A. Imamoglu, and J. Marangos, Rev. Mod. Phys. **77**, 633 (2005).
[2] D. A. Braje, V. Balić, S. Goda, G. Y. Yin, and S. E. Harris, Phys. Rev. Lett. **93**, 183601 (2004).
[3] V. Balić, D. A. Braje, P. Kolchin, G. Y. Yin, and S. E. Harris, Phys. Rev. Lett. **94**, 183601 (2005).
[4] P. Kolchin, S. Du, C. Belthangady, G. Y. Yin, and S. E. Harris, Phys. Rev. Lett. **97**, 113602 (2006).
[5] S. Du, J.-M. Wen, M. H. Rubin, and G. Y. Yin, Phys. Rev. Lett. **98**, 053601 (2007).
[6] S. E. Harris, M. K. Oshman, and R. L. Byer, Phys. Rev. Lett. **18**, 732 (1967).
[7] D. N. Klyshko, *Photons and Nonlinear Optics* (Gordon and Breach, New York, 1988); M. H. Rubin, D. N. Klyshko, Y.-H. Shih, and A. V. Sergienko, Phys. Rev. A **50**, 5122 (1994); Y.-H. Shih, Rep. Prog. Phys. **66**, 1009 (2003).
[8] J.-M. Wen and M. H. Rubin, Phys. Rev. A **74**, 023808 (2006); **74**, 023809 (2006).
[9] S. Du, E. Oh, J.-M. Wen, and M. H. Rubin, Phys. Rev. A **76**, 013803 (2007).
[10] J.-M. Wen, S. Du, and M. H. Rubin, Phys. Rev. A **76**, 013825 (2007).
[11] C. H. Raymond Ooi, Q. Sun, M. S. Zubairy, and M. O. Scully, Phys. Rev. A **75**, 013820 (2007).
[12] P. Kolchin, Phys. Rev. A **75**, 033814 (2007).
[13] S. Du, C. Belthangady, P. Kolchin, G. Y. Yin, and S. E. Harris (unpublished).

[14] J.-M. Wen, S. Du, and M. H. Rubin, Phys. Rev. A **75**, 033809 (2007).
[15] J.-M. Wen, S. Du, M. H. Rubin, and E. Oh, Opt. Express (to be published).
[16] J. D. Franson, Phys. Rev. Lett. **62**, 2205 (1989).
[17] Y. P. Zhang and M. Xiao, Appl. Phys. Lett. **90**, 111104 (2007).
[18] Y. P. Zhang, A. W. Brown, and M. Xiao, Opt. Lett. **32**, 1120 (2007).
[19] Y. P. Zhang, A. W. Brown, and M. Xiao, Phys. Rev. Lett. **99**, 123603 (2007).
[20] A. Joshi and M. Xiao, Phys. Lett. A **317**, 370 (2003); Phys. Rev. A **71**, 041801(R) (2005); **72**, 062319 (2005).
[21] M. O. Scully and M. S. Zubairy, *Quantum Optics* (Cambridge University Press, Cambridge, UK, 1997).
[22] C. H. Raymond Ooi and M. O. Scully, Phys. Rev. A **76**, 043822 (2007).
[23] R. W. Boyd, *Nonlinear Optics* (Academic Press, San Diego, 2003); R. W. Boyd, M. G. Raymer, P. Narum, and D. J. Harter, Phys. Rev. A **24**, 411 (1981).
[24] P. D. Drummond and D. F. Walls, Phys. Rev. A **23**, 2563 (1981); M. D. Reid and D. F. Walls, *ibid.* **34**, 4929 (1986); D. F. Walls and G. J. Milburn, *Quantum Optics* (Springer-Verlag, New York, 1995).
[25] In the laser-cooled atomic gas, the linewidth broadening due to the Doppler effect is very small and is negligible. For example, see experimental demonstrations of paired-photon generation in [3–5].
[26] Choosing the two-level system as an example, the effects of the Langevin noises to the two-photon correlation have been carefully analyzed by M. H. Rubin, J.-M. Wen, and S. Du (unpublished). The same procedure can be extended to the current inverted-Y system. On the other hand, the validity of neglecting Langevin noises in the two-photon correlation in a cascade amplifier has been recently discussed in [22].
[27] M. Xiao, Y.-Q. Li, S.-Z. Jin, and J. Gea-Banacloche, Phys. Rev. Lett. **74**, 666 (1995); J. Gea-Banacloche, Y.-Q. Li, S.-Z. Jin, and M. Xiao, Phys. Rev. A **51**, 576 (1995).
[28] T. B. Pittman, Y. H. Shih, D. V. Strekalov, and A. V. Sergienko, Phys. Rev. A **52**, R3429 (1995).
[29] A. N. Boto, P. Kok, D. S. Abrams, S. L. Braunstein, C. P. Williams, and J. P. Dowling, Phys. Rev. Lett. **85**, 2733 (2000); M. D'Angelo, M. V. Chekhova, and Y. Shih, *ibid.* **87**, 013602 (2001).
[30] For example, M. H. Rubin, Phys. Rev. A **54**, 5349 (1996); E. Brambilla, A. Gatti, M. Bache, and L. A. Lugiato, *ibid.* **69**, 023802 (2004); M. D'Angelo and Y.-H. Shih, Laser Phys. Lett. **2**, 567 (2005); J.-M. Wen, P. Xu, M. H. Rubin, and Y.-H. Shih, Phys. Rev. A **76**, 023828 (2007); J.-M. Wen, M. H. Rubin, and Y.-H. Shih, *ibid.* **76**, 045802 (2007).
[31] H. J. Kimble, M. Dagenais, and L. Mandel, Phys. Rev. Lett. **39**, 691 (1977).